

Electronic Supplementary Information

**Ferroelectric polyoxometalate modified nano semiconductor TiO₂ for
increasing electrons lifetime and inhibiting electrons recombination
in Dye-Sensitized Solar Cells**

Yitong Gu^a, Ting Wang^a, Yi-na Dong^b, He Zhang^a, Di Wu^a and Weilin Chen^{*a}

^aKey Laboratory of Polyoxometalate Science of Ministry of Education Department of Chemistry, Northeast Normal University, Changchun 130024, China.

^bThe Second High School in Mongolian Autonomous County of Qian Gorlos, Songyuan, Jilin 138000

Email: chenwl@nenu.edu.cn.

Table of Contents

Supplementary Experimental Section	S3
1. Photoelectrochemical measurements.....	S3
2. Material characterizations.....	S3
Supplementary Figures.....	S4
Fig. S1 IR of Sm.....	S4
Fig. S2 PXRD patterns of Sm.....	S4
Fig. S3 UV-vis absorption spectra of Sm.....	S4
Fig. S4 EDS spectrum of Sm@TiO ₂ /P25.....	S5

Fig. S5 J-V curves of DSSCs based on different mass concentrations of Sm@TiO ₂ /P25 in the photoanodes.....	S5
Fig. S6 OCVD spectra of DSSCs based on different mass concentrations of Sm@TiO ₂ /P25 in the photoanodes.....	S5
Fig. S7 Bode phase diagrams of DSSCs based on different mass concentrations of Sm@TiO ₂ /P25 in the photoanodes.....	S6
Fig. S8 The EIS spectra of DSSCs based on different mass concentrations of Sm@TiO ₂ /P25 in the photoanodes.....	S6
Fig. S9 The photocurrent response of DSSCs based on different mass concentrations of Sm@TiO ₂ /P25 in the photoanodes.....	S6
Fig. S10 The IPCE of DSSCs based on different mass concentrations of Sm@TiO ₂ /P25 in the photoanodes.....	S7
Fig. S11 Equivalent circuit used to fit the impedance measurements on the DSSCs.....	S7
Fig. S12 Long-term stability of DSSCs based on 5%Sm@TiO ₂ /P25.....	S7
Fig. S13 Dye-loading texts of TiO ₂ and different concentrations of Sm@TiO ₂ /P25 films.....	S8
Table S1. The corresponding dye-loading values of TiO ₂ and different concentrations of Sm@TiO ₂ /P25 films.....	S8

Supplementary Experimental Section

Photoelectrochemical measurements:The photocurrent curve was measured on the CHI601D electrochemical workstation (Shanghai Chenhua Instrument Corp., China) with the solar simulator at room temperature. The Cyclic voltammetry curves were carried out on a CHI601D electrochemical workstation (Shanghai Chenhua Instrument Corp., China) at room temperature by a three-electrode system. Glassy carbon electrode was the working electrode, a standard Ag/AgCl and Pt were reference electrode and counter electrode. The electrolyte was 0.05 mol L⁻¹KCl aqueous solution.

Material characterizations:Bruker AXS TENSOR-27 FTIR spectrometer by KBr pellets was used to test the IR spectra from 4000 cm⁻¹ to 400 cm⁻¹. The datas of Powder X-ray diffraction (XRD) were acquired on a Bruker AXSD8 Advance diffractometer in a 2θ scope of 5-80° at a rate

of 10° depending on Cu Ka radiation ($\lambda = 1.5418 \text{ \AA}$). Scanning electron microscope (SEM), Energy dispersive X-ray (EDX) and Energy dispersive spectroscopy (EDS) spectrometry Element mapping were completed by means of a FEI Quanta 200F microscope involving a 20 kV speeding up voltage. The Transmission electron microscope (TEM) images were performed with accelerating voltage of 200 kV on a JEOL-2100F transmission electron microscope. The XPS was completed on an ESCALAB 250Xi photoelectronic spectrometer of F-doped SnO₂ glass with an internal reference of C1s photoelectron at 284.6 eV peak and an Al Ka radiation X-ray source. The Uv-vis was tested at the spectral range from 200 nm to 900 nm on an Ultraviolet spectrophotometer of China SP-756P. The photoluminescent spectrum (PL) was carried out on a Hitachi F-4500 fluorescence spectrophotometer.

Supplementary Figures

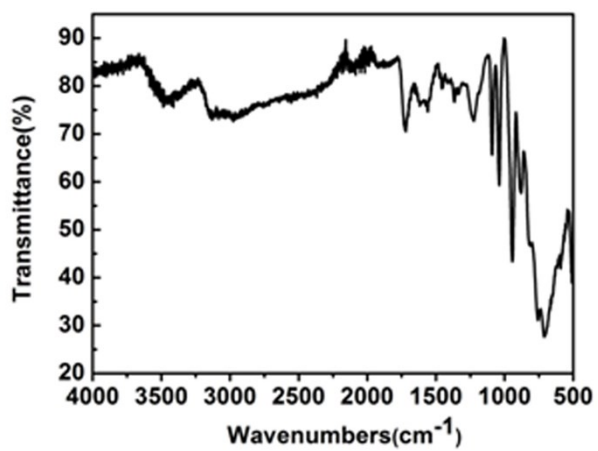


Fig.S1 IR of Sm.

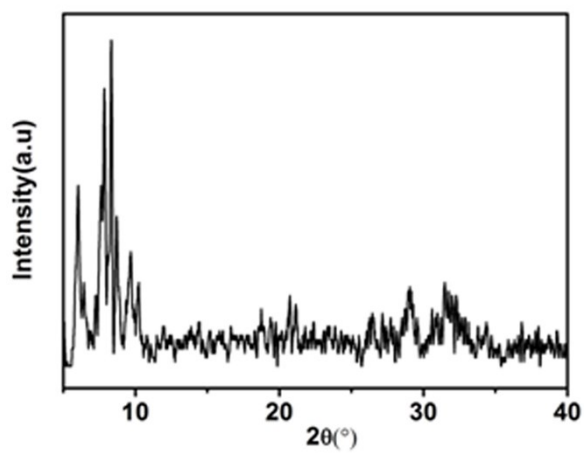


Fig. S2 PXRD patterns of Sm.

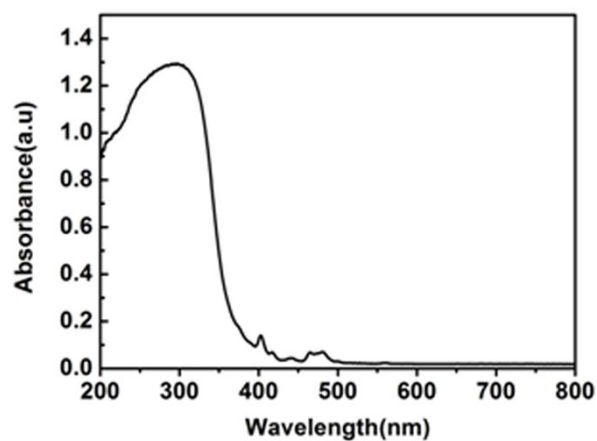


Fig. S3 UV-vis absorption spectra of Sm.

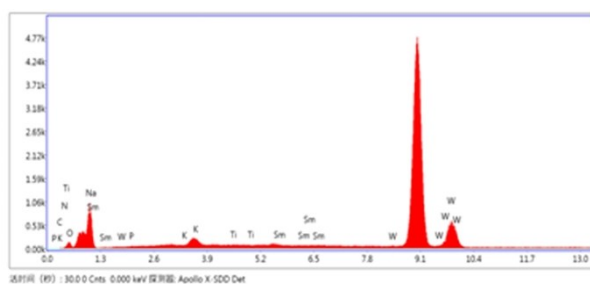


Fig. S4 EDS spectrum of Sm@TiO₂/P25.

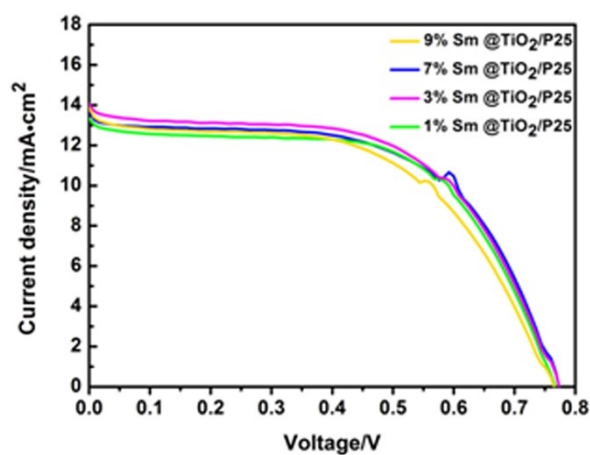


Fig. S5 *J-V* curves of DSSCs based on different mass concentrations of Sm@TiO₂/P25 in the photoanodes.

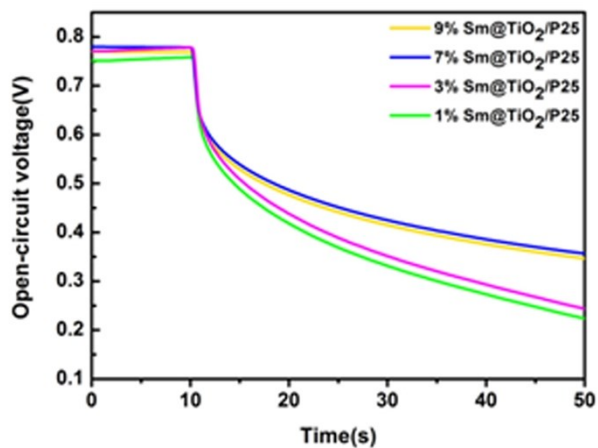


Fig. S6 OCVD spectra of DSSCs based on different mass concentrations of Sm@TiO₂/P25 in the photoanodes.

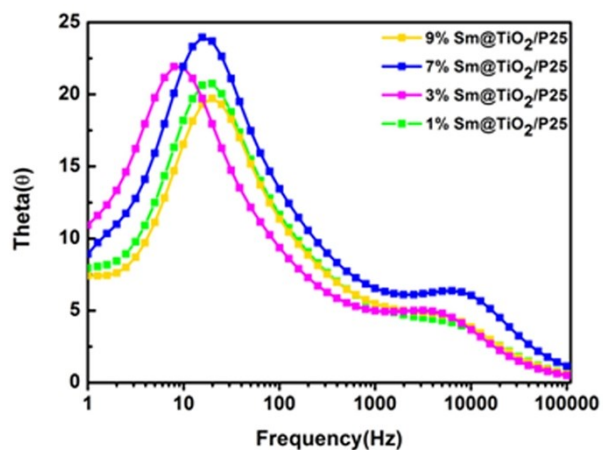


Fig. S7 Bode phase diagrams of DSSCs based on different mass concentrations of Sm@TiO₂/P25 in the photoanodes.

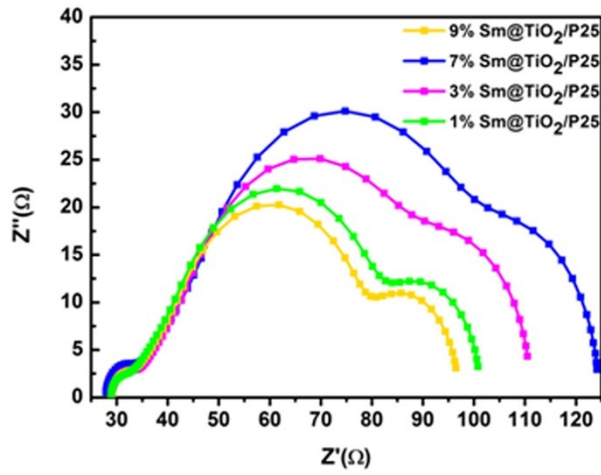


Fig. S8 The EIS spectra of DSSCs based on different mass concentrations of $\text{Sm@TiO}_2/\text{P25}$ in the photoanodes.

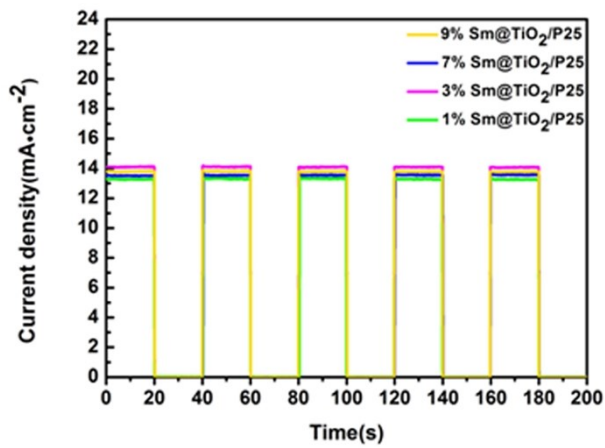


Fig. S9 The photocurrent response of DSSCs based on different mass concentrations of $\text{Sm@TiO}_2/\text{P25}$ in the photoanodes.

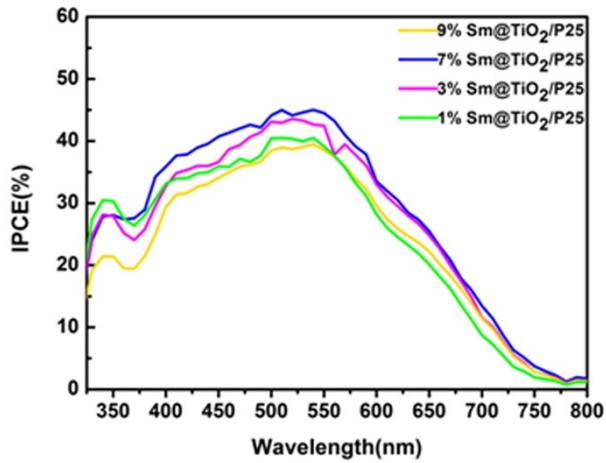


Fig. S10 The IPCE of DSSCs based on different mass concentrations of Sm@TiO₂/P25 in the photoanodes.



Fig. S11 Equivalent circuit used to fit the impedance measurements on the DSSCs.

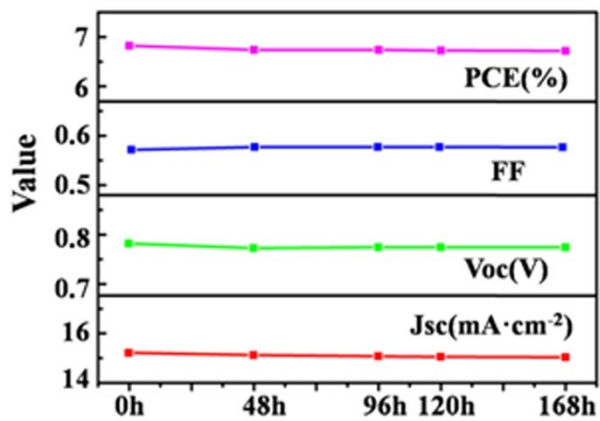


Fig.S12 Long-term stability of DSSCs based on 5%Sm@TiO₂/P25.

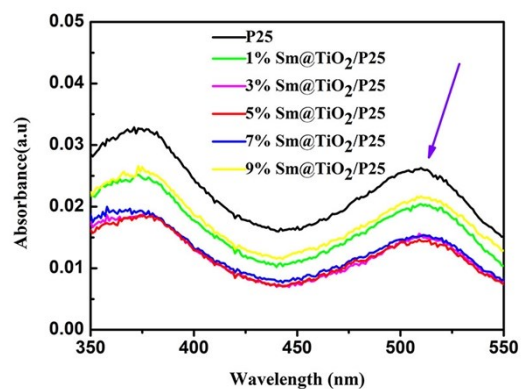


Fig. S13 UV-vis absorption spectrum of TiO₂ and different concentrations of Sm@TiO₂/P25 films.

Table S1 The corresponding dye-loading values of TiO₂ and different concentrations of Sm@TiO₂/P25 films.

Samples	Dye-loading values / mol
TiO ₂	1.862695×10 ⁻⁹
1% Sm@TiO ₂ /P25	1.447660×10 ⁻⁹
3% Sm@TiO ₂ /P25	1.105390×10 ⁻⁹
5% Sm@TiO ₂ /P25	1.041418×10 ⁻⁹
7% Sm@TiO ₂ /P25	1.091844×10 ⁻⁹
9% Sm@TiO ₂ /P25	1.536879×10 ⁻⁹